PHILOSOPHICAL TRANSACTIONS A

rsta.royalsocietypublishing.org

Research

Article submitted to journal

Subject Areas:
wave motion, oceanography, polar regions

Keywords:
ocean waves, sea ice, attenuation, parameterization, power law fluid

Author for correspondence:
Vernon A. Squire
e-mail: vernon.squire@otago.ac.nz

A fresh look at how ocean waves and sea ice interact

Vernon A. Squire[1]

[1]Department of Mathematics and Statistics, University of Otago, PO Box 56, Dunedin 9016, New Zealand

Because of their capacity to alter floe size distribution and concentration and consequently to influence atmosphere-ocean fluxes, there is a compelling justification and demand to assimilate waves into ice/ocean models and earth system models. Similarly, global wave forecasting models like Wavewatch III® need better parameterizations to capture the effects of a sea ice cover such as the marginal ice zone on incoming wave energy. Most parameterizations of wave propagation in sea ice assume without question that the frequency-dependent attenuation which is observed to occur with distance x travelled, is exponential, i.e. $A = A_0 e^{-\alpha x}$. This is the solution of the simple first-order linear ordinary differential equation $\mathrm{d}A/dx = -\alpha A$, which follows from an Airy wave mode ansatz $A \exp i(kx \pm \omega t)$. Yet, in point of fact, it now appears that exponential decay isn't observed consistently and a more general equation of the type $\mathrm{d}A/dx = -\alpha A^n$ is proposed to allow for a broader range of attenuation behaviours.

1. Introduction

Ocean wave propagation into and within sea ice fields is a well-established geophysical research topic that is currently attracting renewed attention, prompted by recent adjustments to Arctic sea ice especially, which are occurring as a result of global climate warming. Indeed, [1] and [2] include exhaustive bibliographies that catalog early progress in the field including commentary from the heroic era of exploration [3,4]; experimental studies in the 1930s; the introduction of mathematical sophistication in the 50s and late 60s; the influential work of Wadhams and his collaborators in the 70s and 80s — the latter prompted by the MIZEX campaign, see e.g. [5,6] and papers referenced therein; and more recent further developments utilizing powerful theoretical and numerical solution methods that began with [7] for shore fast sea ice and [8] for finite ice floes such as those found in the marginal ice zone (MIZ).

THE ROYAL SOCIETY PUBLISHING

As well as observations collected in situ, remote sensing has also provided valuable data sets utilizing both satellites and aircraft missions. Whether focused upon continuous pack ice, the loosely compacted ice floes of the MIZ, or pancake ice, nilas, frazil and grease ice, the compilation of research papers and reports is impressive and continues to grow as the contemporary importance of the subject is recognized and technological advances make practicable more sophisticated measurements that were not feasible 20 years ago.

Ocean waves propagating in an ice field are observed to decrease in amplitude. The observed reduction is due to a combination of two processes — scattering and dissipation, which both need to be accommodated in any earth system model, ice/ocean model or wave forecasting parameterization. Scattering redistributes energy but does not eliminate it while dissipation, insofar as the waves are concerned, removes energy. Undoubtedly, the latter process actually reassigns the energy to other parts of the atmosphere/ice/water system, e.g. to kinetic energy in the mixed layer, etc., and this will be important in earth system models which are required to conserve energy because they compute results over very long timescales. However, this prerequisite is not important here, as the system under consideration isn't closed.

The energy transport equation, or the wave action equation in Wavewatch III® where ocean currents are included, is used to embed ocean waves in these large scale models. Here we express this equation in its simplest notional form for energy density $E = E(\mathbf{x}, \omega, \theta)$,

$$(\partial_t + \mathbf{c}_g.\nabla)E = \sum S = S_{\text{in}} + S_{\text{nl}} + S_{\text{ds}} + S_{\text{ice}}, \tag{1.1}$$

where $\mathbf{x}$ denotes the spatial coordinates, ω is the radian frequency $(= 2\pi f = 2\pi/T$ where f is the frequency and T is wave period), θ is the direction of travel of the wave, the group velocity c_g is taken as constant, and $\sum S$ encapsulates a number of source/sink terms, as follows. S_{in} represents wind-wave interaction, S_{ln} is a nonlinear wave-wave interactions' term, S_{ds} is a dissipation (whitecapping) term and $S_{\text{ice}} = S_{\text{ice}}(\mathbf{x}, \omega, \theta)$ is the term of interest in this work as it characterizes how the waves are affected by the ice field. S_{ice} can be partitioned into the two processes introduced above, which are respectively designated attenuation coefficients α_{scat} and α_{dis},

$$S_{\text{ice}} = -c_g\left(E(\alpha_{\text{scat}} + \alpha_{\text{dis}}) + \int_0^{2\pi} EK(\theta - \theta')\,\mathrm{d}\theta'\right), \tag{1.2}$$

$$\text{such that} \quad \int_0^{2\pi} S_{\text{ice}}\,\mathrm{d}\theta = 0 \quad \text{and} \quad -\alpha_{\text{scat}} + \int_0^{2\pi} K(\theta - \theta')\,\mathrm{d}\theta' = 0 \quad \text{when} \quad \alpha_{\text{dis}} = 0.$$

Considerable modelling work has been done to understand α_{scat} in the MIZ, e.g. the phase-resolving, two-dimensional scattering theory described in [9,10] and tested against field data in [11]. The most appreciable scattering occurs when floe diameters and ocean wavelengths are of similar order, so waves passing through a field of pancake ice will not be scattered to any extent. Although, it is recognized that such scattering models are never perfect, the author feels that the redistribution of wave energy that occurs due to scattering which results in attenuation of the wave field expressed through the coefficient α_{scat} is well understood and well modelled. This is important because contemporary phase-resolving scattering models provide a direct link to ice floe breakup and hence to how the floe size distribution changes, as flexural stresses in the compliant ice floes that make up the MIZ are easily calculated [10]. It only remains to find a numerically efficient way to replicate the properties of $K(\theta - \theta')$ in equation (1.2).

Unfortunately, the author cannot say the same in regard to α_{dis}, for which no satisfactory models exist. Dissipation is due to an abundance of processes that are symptomatic of a MIZ, defined as being the region of the ice cover that is substantially affected by open ocean processes. As such, we expect considerable turbulence; inelastic ice floe collisions that can include reducing the ice to a slurry by pummelling; vortex shedding; wave breaking, overtopping and overwashing of the floes and possible green water; energy loss associated with ice deformation under extreme conditions; ridging, rafting and ice floe fracture; and no doubt other less obvious mechanisms.

Near the ice edge, when the seas are rough, considerable destruction of the ice floes can occur but, because the dissipation eliminates higher frequency waves before lower frequency ones, the zone of intense energy loss is typically limited to 10 or 20 km or so in Arctic waters, see e.g. [12]. In the Southern Ocean, where seas are much fiercer, the zone of destruction will be considerably broader. It is quite likely that the attenuation rates in these outer zones may deviate significantly from those in the interior and may even have a different functional dependence on the distance travelled by the waves. It is also conjectured that large amplitude waves may attenuate differently from those with smaller amplitudes, as the effects of nonlinear dissipation mechanisms such as overwash and wave breaking will be more pronounced.

Creating a viable model that fits the multifarious realizations of the MIZ is unlikely to be achievable, as the contribution from these several dissipative mechanisms will change with both the wave and the ice conditions. Moreover, although the scattered fields are reasonably well understood as noted above, potentially very energetic dissipation will also occur in the waters between floes as a result of the scattering process itself. The convenience of separating α_{scat} and α_{dis} in equation (1.2) may be problematical in this regard, although we accept its utility. Nonetheless, while its magnitude may change according to ice conditions, in field observations a simple power law appears to describe consistently how attenuation changes with wave frequency. To the author's knowledge, no model has reproduced this proportionality yet unfortunately; indeed most are way off the mark and it is unlikely that a linear model will ever accurately reproduce what is observed.

The above comments notwithstanding, it is conspicuous that the vast bulk of theoretical models constructed to describe how waves are affected by sea ice, or vice versa, are configured to fit a linear paradigm, i.e. they employ an Airy wave mode ansatz [13] of the form $A \exp i(kx \pm \omega t)$. In this expression, A is the initial wave amplitude, k denotes a generic complex wave number that here defines either propagation in the water or beneath the ice cover, x is the direction of propagation and t is time. In the usual way, $k = \kappa + i\alpha$ encapsulates dispersion (via the real quantity κ) and attenuation (via imaginary $i\alpha$) into one consolidated complex wave number. Typically, a boundary value problem is then solved, e.g. for open water surface gravity waves travelling into an homogeneous plate or layer which can be semi-infinite or finite in horizonal extent and has prescribed physical properties that define its behaviour in flexure. As a rule, the ice would be designated as elastic, viscous or viscoelastic; each being reasonable when the wave amplitudes are modest for the strain rates induced by typical surface waves in the sea ice under different circumstances. The material properties chosen for the ice provide the dispersion relation that regulates how the waves propagate under the ice cover, i.e. how they disperse and reduce in amplitude, and, because the wave numbers in open water and ice-covered sea are different, the impedance change at the ice edge which causes some of the wave energy to be reflected. Weakly nonlinear formulations exist but they are relatively rare, e.g. [14].

In case the reader misunderstands, I am not dismissing the use of linear models to describe wave propagation into and through sea ice fields. Indeed, the author along with graduate students and colleagues has constructed many linear, physically-based models to describe complex wave-ice interactions, notably [7–10] for example, over many years. Rather, I am cautioning that the a priori adherence to the linear $A = A_0 e^{-\alpha x}$ prototype is problematical when (i) parameterizing in operational forecasting systems and earth system models, as it predisposes the attenuation to be exponential; (ii) attempting to fit any such model to data, because the exponential function $A = A_0 e^{-\alpha x}$ may have too few degrees-of-freedom to fit the data at all the spectral wave frequencies present. Moreover, (ii) may contribute to unexplainable data artefacts documented in some published work, which have justifiably been attributed to wave growth or wave-wave interactions in the past that are sometimes evident but not always present [6,15].

2. Appraisal

(a) Two paradigms

A crucial distinction needs to be made between two classes of theoretical model, designated paradigms I and II herein. Articles [7–10] are paradigm I examples of models where the physics of wave-ice interaction is replicated theoretically as credibly as possible. In the first paper, [7] solve for the reflection and transmission coefficients at the interface between an open water half-space and a half-space covered by a uniform ice sheet that represents so-called shore fast sea ice. In concert with many models describing how ice flexes in response to waves, [7] assumes the ice responds as a thin elastic plate. [8] also computes reflection and transmission coefficients, but this time for a finite elastic ice floe. In the third example [9], a MIZ bathed by a prescribed directional wave spectrum is modelled by means of large numbers of floating compliant plates which scatter the penetrant wave energy in all directions. [10], the fourth example, leads on from [9], using its scattering theory to evolve the MIZ floe size distribution, by breaking up those ice floes that are too large to exist in the wave field using a Mohr-Coulomb fracture criterion. In all cases, the physical properties of the ice, viz. its thickness, ice density and the elastic moduli, etc., can be mapped straightforwardly onto the coefficients that appear in the model and in situ experiments can be done to ascertain whether the model is a good fit to data. It is these attributes that are symptomatic of a paradigm I model.

On the other hand, some theoretical work is more accurately labelled as a parameterization and fits paradigm II, including models that are constructed for one purpose being used for another. I am not dismissing the value of paradigm II, as it is simply not practicable to incorporate fully phase-resolving wave-ice interaction theory into either an earth system model or Wavewatch III®; a pragmatical solution is therefore necessary that parameterizes the physics in the most accurate way. Potential examples in current use are the viscoelastic layer of [16], which is well suited to modelling waves travelling in homogeneous continuous ice, or the modified fast ice model $[7]^{\mu}$ altered to have a complex flexural rigidity so as to produce damping, being used to model an entire, potentially open, i.e. of low-concentration, heterogeneous ice field. (The superscript μ denotes viscosity, added to acknowledge that I am referring to a viscoelastic version of the original elastic paper [7].) Parameterization aspires to represent a substantial region of ice cover composed of many ice floes and ice cakes present at spatially-variable concentrations and thicknesses as an *effective* medium with a single dispersion relation that describes how the waves disperse and attenuate as they propagate via the wave number. Zones with different physical properties can be introduced, recalling that the impedance alters where properties change so that a boundary value problem exists at each interface which strictly requires reflection and transmission coefficients to be found. However, the real challenge is mapping a loosely-configured, heterogeneous array of independent ice floes, ice cakes and frazil onto the physical material coefficients that appear in the "holistic" dispersion relation that describes the effective medium. Unlike when the examples [7–10,16] given above are used as originally intended, there is no way that this can be done by independently measuring each physical property of the sea ice and the only recourse is to measure how the waves change as they pass through the ice medium and then to tune the model parameters to "best fit" the observed data. Accordingly, the model is being calibrated with the very data it is intended to predict.

The computed model parameters also strictly have no material physical interpretation as they are only associated with the experimental data being analysed, so generalization to other ice fields or ocean wave states is challenging or impossible. Moreover, it must be asked how faithful the model is to the physics of the process being observed and whether it is actually capable of replicating observations. The author contends that this has not been convincingly demonstrated to date. Indeed, there are incontestable analyses that suggest that $[7]^{\mu}$ and [16] can never replicate observations well as a paradigm II stratagem because their asymptotic behaviour at mid- to high-frequencies is usually wrong and the same is true of viscous layer models such as [17].

Without knowing that they are a universally valid parameterization, some prototype models are already being embedded within operational wave forecasting systems such as Wavewatch III® and earth system models that operate under a very diverse range of environmental circumstances, e.g. for large wave steepnesses where the differential equation predicting attenuation, namely $\mathrm{d}_x A = -\alpha A$ with solution $A = A_0 e^{-\alpha x}$, is unlikely to be a reliable approximation to Nature in all circumstances and the issue of poor adherence to observed $\alpha(\omega)$ behaviour at high frequencies is becoming clear. (Here and subsequently the abbreviation $\mathrm{d}_x \equiv \mathrm{d}/\mathrm{d}x$ is used.)

Although the purpose of this paper is not to review the field of wave-ice interactions, it would be remiss of me not to corroborate the assertions I have made as best I can. This will be done in later sections. Subsequently, using data from a recent field experiment, I will focus on the constraints implicit in linear models that conflate dispersion and attenuation in ice fields using the single complex wave number $k = \kappa + i\alpha$. An alternative differential equation, namely $\mathrm{d}_x A = -\alpha A^n$, derived using physical arguments for pancake ice in [18] and potentially having an additional degree-of-freedom n, will also be presented as a generalization of the archtypal exponential attenuation law $A = A_0 e^{-\alpha x}$. Remarkably, [18]'s model affords the same equation for attenuation built from different physics by [19]. While the physical basis of [19] can be challenged, the differential equation that parameterizes how wave amplitude A changes from its value A_0 at the ice edge as the wave advances through the ice medium, viz.

$$\mathrm{d}_x A = -\alpha A^n \quad \text{with solution} \quad A^{(1-n)} = A_0^{(1-n)} - (1-n)\alpha x, \tag{2.1}$$

where n and α are to be found, is a generalized decay law that reverts to a linear law when $n = 0$ and exponential decay when $n = 1$ [18,19]. The equation is a consequence of allowing viscosity to depend on strain rate and, because of this, frequency ω, in a particular way and derives from a power law fluid constitutive relation. Rather than just "best fit" observations, I will also describe how the value of n can be predetermined to some extent using aggregated intelligence about the nature of wave-ice interaction in MIZs.

(b) Contemporary parameterization

I briefly discuss the three most common material descriptions used to categorize sea ice when it is subjected to ocean wave forcing; elastic, viscous and viscoelastic. The common theme is (i) linearization about the basic state of rest, (ii) assuming the motion is proportional to $A \exp i(kx \pm \omega t)$, and (iii) derivation of a dispersion equation that connects ω with k. The dispersion relations, $\omega = \omega(k)$, are distinct in each case and for different models but the dependency of the amplitude A on x that follows is always exponential.

The generic ice wave number k is real when the ice is purely elastic if no further dissipation, arising from a combination of ice flexing, dissipation in the water and mechanical energy loss such as collisions between ice floes or cakes, is parameterized. Waves disperse differently under solid ice compared to open water and also attenuate because of scattering. This is because the ice-coupled wave number depends on the physical properties of the sea ice so transitions of ice morphology, e.g. thickness, or the edges of ice floes cause reflections to occur. However, this process represents a redistribution of energy as opposed to dissipation. What this means in the context of this paper is that a perfectly elastic sea ice cover can only reduce wave amplitude if the ice is not spatially uniform.

A number of papers represent the entire sea ice cover as a viscous layer at the ocean surface, e.g. [17] models wave propagation in a Newtonian viscous layer floating on an inviscid ocean, while in [20] the underlying ocean is allowed to be viscous too. The primary focus of [17]'s model was to explain some laboratory observations on wave propagation in grease ice written up subsequently by [21], whereas [20] applied their model to a broader range of ice types including the MIZ. Using a Lagrangian formulation, [22] also constructed a viscous model — in this case for an unlayered, rotating ocean, and used it to represent a MIZ. [23] and [24,25] used a viscous boundary layer model, based upon the eddy viscosity in the turbulent boundary layer beneath the ice cover, observing that eddy viscosity is a phenomenological parameter that is to be determined as a function of flow conditions rather than a physical measurable viscosity. These few papers collectively illustrate a reasonably common way of parameterizing the aggregated effect of sea ice on waves.

In fact, sea ice itself is viscoelastic, with different degrees of nonlinearity dependent on its physical properties and environmental circumstances. At ocean wave forcing frequencies, first-year sea ice itself is approximately anelastic [26], i.e. any viscous deformation is recoverable, which is a specific form of viscoelasticity where the hysteresis loop is closed. However, current viscoelastic plate [27] and viscoelastic layer [16,28–30] models — the latter originally built to synthesize the elastic plate [7] and viscous layer model [17], ignore this subtlety. Instead, they accommodate other kinds of sea ice deformation and/or alternative dissipative mechanisms that cause energy loss as the waves propagate into and through the material. In doing this they are including both the modest dissipation due to sea ice flexure plus the typically substantial energy loss arising from the several known but neglected pervasive mechanisms discussed in §1 — many of which are nonlinear but are being rendered in a linear way in the model. In all cases, a dispersion relation $\omega = \omega(k)$ results that, as usual, is constructed by first assuming the Airy wave mode ansatz $A \exp i(kx \pm \omega t)$ with $\kappa = \operatorname{Re} k$ expressing dispersion and $\alpha = \operatorname{Im} k$ expressing attenuation via $A = A_0 e^{-\alpha x}$ so any nonlinearity is neglected a priori.

It is also noteworthy that variations in concentration c are treated by reducing the effective medium's effect linearly. At first sight this seems reasonable but, when it is recognized that most of the dissipation arises because of turbulence in the water, it becomes counterintuitive. Surely the level of dissipation would increase initially with a reduction in c, as ice floes become more mobile and "belligerent", and then start to decrease as $c \to 0$ as the effects of floe collisions, waves breaking over floes and overwashing, and less attenuation, subside.

Observations suggest that $\alpha(\omega) \propto \omega^2$–$\omega^3$ in many circumstances, yet Dr Johannes Mosig (personal communication, 2017) has shown, after switching off any elasticity, that $[7]^{\mu}$ and [17] have power 11 and power 7 proportionality respectively. The dispersion relation in [16] is so complicated that it is hard to be absolutely sure about its asymptotic behaviour but with zero shear modulus it is expected to behave like the Keller model [17], so is likely to be power 7 as well. All enhanced viscosity ocean models [22–25] go as $\omega^{7/2}$. The closest to ω^2–ω^3 to date is [7], for which $\alpha(\omega) \propto \omega^3$. It has simple velocity-dependent damping incorporated in the elastic plate model [7] as an alternative to the flexural rigidity being made complex as in $[7]^{\mu}$. This is well illustrated in Figure 1, which shows wave spectra from a 2015 field experiment in the Beaufort Sea carried out from the ship R/V Sikuliaq. In Figure 1 these data are compared with Wavewatch III® modelled hindcasts, based upon [16] but with the shear modulus set to zero making it equivalent to the model in [17]. The figure indicates that the model is damping high frequency energy strongly in all cases, while the buoys indicate that strong damping is occurring only for a subset of cases. Presumably, $\alpha(\omega) \propto \omega^7$ behaviour is responsible for the high frequency tail drop off that is so evident in the dashed red and green theoretical curves but is absent in the solid red and green data curves. The corresponding blue curves, which arise from higher concentrations of pancakes and frazil, both do decrease rapidly at first on the other hand. A more general equation describing attenuation such as $\mathrm{d}_x A = -\alpha A^n$ built into Wavewatch III® could allow for such variations.

3. The power law model

(a) A granular floe jostling model

To the author's knowledge, the differential equation $\mathrm{d}_x A = -\alpha A^n$ was first applied to sea ice back in 1973 [19], specifically invoking a model of dissipation based on the Glen-Nye flow law for glacial steady-state flow, where $n = 3$. In its general form the equation requires that the viscosity of the deforming material μ is not constant, as it would be for Newtonian flow, but that it depends on strain rate. When $n = 3$, $\mu(\cdot)$ is inversely proportional to the square of $J_2 = \sqrt{\frac{1}{2}\sigma_{ij}^{(d)}\sigma_{ij}^{(d)}} = \tau$, which is defined as the second invariant of the deviatoric stress tensor

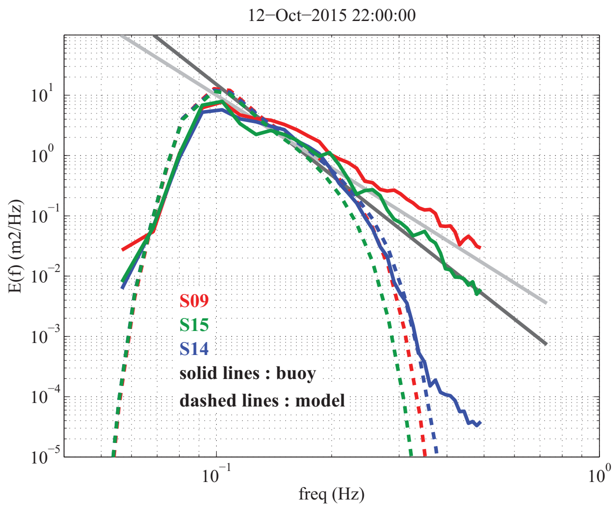

Figure 1. Example comparisons of one dimensional wave spectra for three different SWIFT buoys, corresponding to the same time (2200 UTC 12 October 2015). Dark and light gray lines correspond to an $f^5(\omega^5)$ and $f^4(\omega^4)$ tail slope, respectively. Solid red, dark green, and blue lines are measured spectra. Corresponding dashed lines are from model hindcasts. After [15].

$\sigma_{ij}^{(d)}$, but when n is unspecified $\mu(\cdot) \propto \tau^{(1-n)}$. The quantity τ is called the effective shear stress or octahedral stress. Physically, a choice of $n = 3$ is hard to justify as anything other than a parameterization characterizing the synthesis of all of the dissipative processes effected on ocean wave trains as they propagate within a MIZ, because there is no physical argument that can explain why waves should lose energy in the same manner as a creeping glacier. The strain rates associated with the two natural phenomena are different by several orders of magnitude. Yet the model did rather well in replicating observations in both the Arctic and Antarctic MIZs [19].

Nonetheless, although serendipitous, a back-of-the-envelope analysis of pancake ice subjected to waves that invokes granular flow theory [18], also produces the same equation, i.e. $\mathrm{d}_x A = -\alpha A^n$. The differential equation actually arises from the so-called power-law fluid, which is defined such that

$$\sigma_{ij}^{(d)} = 2\mu(\cdot)\dot{\epsilon}_{ij} = 2\left(\tfrac{1}{2}M^{-1}\tau^{(1-n)}\right)\dot{\epsilon}_{ij} = 2\left(\tfrac{1}{2}M^{-\frac{1}{n}}\dot{\epsilon}^{\frac{1-n}{n}}\right)\dot{\epsilon}_{ij}, \tag{3.1}$$

where M is constant, $\dot{\epsilon}_{ij}$ is the strain rate tensor and $\dot{\epsilon} = \sqrt{\frac{1}{2}\dot{\epsilon_{ij}}\dot{\epsilon_{ij}}}$ is effective strain rate.

Power-law fluids have a strain-rate-dependent apparent viscosity $\mu(\cdot) \propto \dot{\epsilon}^{\frac{1-n}{n}}$. The value that the index n takes on determines the way the material deforms; for example, when $n \in (0, 1)$, $\mu(\cdot)$ increases with increasing strain rate and it is said to be dilatant or shear thickening; when $n \notin (0, 1)$, the viscosity $\mu(\cdot)$ decreases as strain rate increases and the material is described as pseudoplastic or shear thinning. Because shorter period waves reduce in amplitude more rapidly than longer ones in sea ice, i.e. attenuation increases as frequency and strain rate increase, the phenomenon of wave-ice interaction is dilatant. This does not, however, necessarily mean that sea ice is a dilatant material; indeed at very long timescales it would be expected to behave similarly to fresh water glacial ice and to be pseudoplastic. To the author's knowledge the power law fluid has not been considered as a viable constitutive relation for sea ice itself.

Interestingly, dilatancy has the special cases (i) $n = 0$, where viscosity μ increases linearly with τ, which leads to the imperative of waves decaying linearly in the present context; (ii) $n = 1/2$, where μ increases linearly with $\dot{\epsilon}$; and (iii) $n = 1$, where $\mu = \text{const.}$ and an exponential decay law holds. Of course, n can take on other values that determine whether the attenuation is less or more rapid than exponential.

(b) Choosing n

In §2(b) I observed that several models describe wave propagation in the MIZ by making the ocean more viscous there, typically through the use of an eddy viscosity that captures the enhanced internal fluid friction arising from the turbulent transfer of momentum by eddies analogous to the action of molecular viscosity in laminar flow but on a much larger scale. These models have a dispersion relation of the form $\mu g^2 k^4 = 2\omega(\omega^2 - gk)^2$ and furnish an $\alpha(\omega) \propto \omega^{7/2}$. By way of a demonstration, I ask the question "can $\mu(\cdot)$ be adjusted such that the order of these viscous models is reduced from $\omega^{7/2}$ to ω^2 by choosing n such that the excessive dilatancy is eliminated?". It is conjectured that $n = -2$ achieves this goal, ultimately producing $\alpha(\omega) \propto \omega^2$ from that predicted by the dispersion relation.

Also, by way of illustration, we can investigate how a plausible amplitude spectrum $A_0(f)$ evolves with distance x, again assuming that $\alpha(f) \propto f^2$ recalling that $\omega = 2\pi f$. $A_0(f)$ is derived from the quintessential Pierson-Moskowitz spectrum $E_0 = E_0(f)$ at the ice edge by integrating across a comb of frequency bands. E_0, see Figure 2(*a*), has the form

$$E_0(f) = 8.1 \times 10^{-3} \frac{g^2}{(2\pi)^4} f^{-5} \exp\left(-\frac{5}{4}\left(\frac{f_{\rm p}}{f}\right)^4\right), \tag{3.2}$$

where $f_{\rm p}$ is the peak frequency which is set to 0.1 Hz to be consistent with Figure 1, g is the acceleration due to gravity, and the numerical constant 8.1×10^{-3} is known as the Phillips constant [31]. Equation (3.2) can be integrated to give $\int E_0(f)\,\mathrm{d}f = \exp\left(-1.25 \times 10^{-4} f^{-4}\right)$, so it is an easy matter to create A_0 directly or by numerical integration. The two sets of amplitude spectra, coloured green, magenta and yellow in Figures 2(*b*) and 2(*c*) show the frequency-dependent attenuation experienced by the $A_0(f)$ spectrum as it advances into the notional ice cover which either attenuates exponentially (*b*) or linearly (*c*) with penetration x. It is very evident that the linear decay (*c*) is much greater for the same constant of proportionality in $\alpha \propto f^2$. Although an artificial experiment, it does demonstrate the potential of the more general behaviour furnished by $\mathrm{d}_x A = -\alpha A^n$, which may be especially useful for parameterizing dissipation caused by the aggregation of nonlinear processes that expunge energy from incoming wave trains for the first ten or so kilometres from the ice edge or, in all likelihood, farther when wave amplitudes are large (see §1).

Finally, let us consider some real data and adopt the red curve in Figure 1 which shows that the outer energy density $E_0(f)$ has an f^{-4} tail above $f = 0.1$ Hz, i.e. $E_0(f) \propto f^{-4} \implies A_0(f) \propto f^{-2}$. (The Pierson-Moskowitz spectrum has an f^{-5} tail and we have confirmed that the $A_0(f)$ spectrum in Figures 2(*b*) and 2(*c*) has an $f^{-\frac{5}{2}}$ tail, as required.) Seek a model that has an $\alpha(f) \propto f^2$ form irrespective of the value of n, interpreting α throughout equivalently. Three examples are considered, the first of which is somewhat artificial, as follows

(i) Suppose that the f^{-4} tail in the spectrum doesn't change as the wave field from which it is constituted propagates farther into the sea ice cover. Using equation (2.1) it is straightforward to argue that $n = 2$ is the only value of n that can produce the desired behaviour for α at frequencies above about 0.1 Hz. For $n = 2$, $\alpha = (A^{-1} - A_0^{-1})/x$.

(ii) Exponential attenuation is recovered when $n = 1$. In this case, amplitude $A = A_0 \exp(-\alpha x) \propto f^{-2} \exp(-\alpha x) = f^{-2}(1 - \alpha x + \ldots)$, so that $A \underset{\sim}{\propto} f^{-2}(1 - c_1 f^2 x)$ to first order, i.e. an initial linear decay.

(iii) For the linear attenuation case, viz. $n = 0$, $A = A_0 - \alpha x \propto f^{-2}(1 - c_2 f^4 x)$.

In the above c_1 and c_2 are constants that arise from the proportionalities assumed, i.e. in the tail of the incident energy density spectrum, where $E_0(f) \propto f^{-4}$, and $\alpha(f) \propto f^2$. Although the exponential case is initially linear, the degree to which the amplitude reduces as a function of distance x travelled is greater for the linear attenuation example if the magnitudes of α are similar, as observed in the Pierson-Moskowitz analysis reported above.

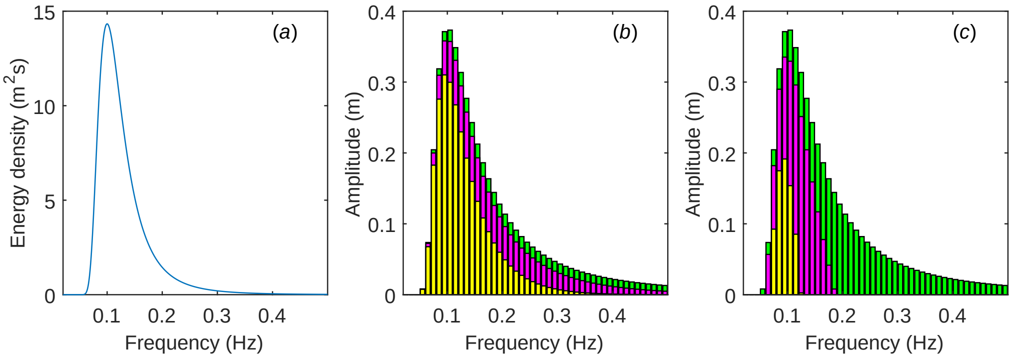

Figure 2. ((*a*) The Pierson-Moskowitz spectrum E_0 defined by equation (3.2). *(b)* The partially obscured green bar graph is an amplitude spectrum $A_0(f)$ created from $E_0(f)$ by integrating across frequency bands of width 0.01 Hz with the central frequency at the mid-point. $A_0(f)$ is plotted as a bar graph to emphasize that each amplitude is valid over a frequency band, e.g. from 0.2–0.21 Hz with a central frequency 0.205 Hz, rather than at a single frequency. The other amplitude spectra, coloured magenta and yellow respectively, show how A_0 evolves exponentially, i.e. when $n = 1$, as x increases. *(c)* Amplitude spectra constructed in the same manner as for *(b)*, but for $n = 0$, i.e. linear attenuation. Identical values for the constant of proportionality in $\alpha \propto f^2$ and the distances from the ice edge are used for *(b)* and *(c)*, chosen to emphasize the disparity between exponential and linear attenuation. It is the relativity between the same colours in plots *(b)* and *(c)* that is important, rather than the absolute values.

(c) Limiting cases

There has been a some evidence presented in observations [32] that the gradual, frequency-dependent reduction in the amplitude of ocean waves with distance travelled may be linear as opposed to exponential, under some circumstances and particularly when the waves are of substantial amplitude. Although this has been disputed subsequently [33] in the context of [32], it is of interest to establish whether such a form of attenuation occurred in the 2015 R/V Sikuliaq data set, where the wave amplitudes were large during some experiments as this accords with our original conjecture in §1. This is illustrated for a single wave attenuation experiment which took place from 11$^{\text{th}}$ to 13$^{\text{th}}$ October 2015 in Figure 3, where the median n value extracted from a direct best fit of the data is plotted against energy density in plot 3(*a*), median n is plotted against the mean value of frequency in plot 3(*b*), and the percentage of linear attenuation profiles as a function of energy density is plotted in plot 3(*c*). It is quite clear that the likelihood of a profile being linear, i.e. $n = 0$, increases with the energy density and hence wave amplitude from plot 3(*a*). It is also clear from plot 3(*b*) that $n = 0$ is associated with low frequencies but this is simply because of the shape of the wave spectrum entering the ice field, which goes as f^{-4} in the part of the spectrum where significant energy exists. The percentage of $n = 0$ decay profiles increases monotonically with the energy density, flattering out at about 60% or so beyond an energy density E_0 of about 5 m^{2}s as shown in plot 3(*c*). Consequently, the author contends that ocean waves do sometimes decay linearly during their passage through sea ice fields and that this should be accommodated in models such as Wavewatch III$^{®}$, which are used in forecasting where high fidelity outputs can matter.

A similar analysis can be done with significant wave height in the manner of [32], which produces an analogous conclusion, namely that waves are most likely to attenuate exponentially when they are of modest amplitude but to attenuate linearly when they reach a predefined critical value that will depend on the properties of the ice field through which the waves are propagating.

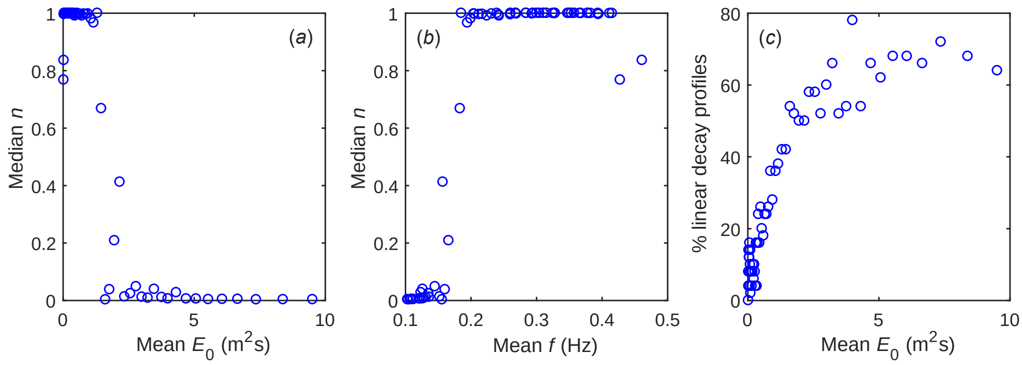

Figure 3. Left panels show n versus E_0, created from clusters of E_0 that each contain about 100 estimated values. Each point on the plot gives the mean of this sample of E_0 values versus the median of the corresponding sample of n values. The transition between $n = 1$ and $n = 0$ occurs at $E_0 \sim 1.5\,\mathrm{m}^2\mathrm{s}$. The median of n versus the mean of the frequency calculated as the mean of all the frequency samples corresponding to the E_0 samples in a bin is shown in the middle panels. There is a dependence on frequency which follows closely the dependence on energy because the two are strongly correlated for $f > 0.1$ Hz in the spectral tail where $E_0 \propto f^{-4}$. The right panels show the percentage of linearly decaying profiles in each E_0 bin.

4. Summary

To finish, the most significant conclusions of this paper are drawn together here, as follows

(i) It is not feasible to use a paradigm I model in a global scale earth system model or Wavewatch III®.
(ii) The reduction in amplitude observed in ocean waves travelling through sea ice is due to two phenomena; conservative scattering by the ice floes, which relocates energy, and true dissipation, arising from copious nonlinear phenomena which remove energy that are poorly understood and modelled.
(iii) Dissipation is likely to be extreme closest to the ice edge and/or when the waves are most fierce but the width of the zone over which it dominates other sources of attenuation will vary with the wave and ice conditions and it is probable that the most severe environments will occur in the Southern Ocean as a result.
(iv) Scattering is most significant when the diameter of the ice floes is of the same order as wavelength, while dissipation is always present but likely to be less important when wavelengths are larger.
(v) Although the energy transport equation's source/sink term S_{ice}, defined in equation (1.2), separates α_{scat} and α_{dis}, the scattered wave field will also be subjected to considerable dissipation that will reduce its impact on surrounding floes.
(vi) Ocean waves break up ice floes, a process that is modelled well by scattering theory which takes into account the flexural stresses in the floes that are provoked by wave-induced bending.
(vii) Nearly all contemporary models constructed to characterize wave propagation into and beneath sea ice in its several forms are linear and all paradigm II models are linear with some having been reapplied to represent "effective media" in circumstances that they were not originally intended to model.
(viii) The fidelity of current effective media models in the MIZ has not yet been demonstrated.
(ix) Material constants in effective media have no physical meaning, as to make its predictions the medium aggregates a smorgasbord of disparate mechanisms and calibration is unattainable because of the unique set of conditions that define each experiment.
(x) Observations indicate that the attenuation coefficient α has a power law frequency dependence of the form $\alpha(\omega) \propto \omega^p$, where $2 \leq p \leq 3$, with several experiments giving

$p = 2$, yet parameterizations created from contemporary linear models do not nearly reproduce the asymptotic details observed in field observations for p.

(xi) Primarily because of dissipation, there is reasonable observational evidence to conclude that attenuation is not always exponential and a natural consequence of this is that waves may experience different "attenuation laws", during their passage through ice fields.

(xii) Because of nonlinearity, exponential attenuation appears to be associated with waves of low amplitude while higher waves may be attenuated linearly.

(xiii) Scaling the material constants linearly to absorb concentration changes is counterfactual.

(xiv) The decay law $\mathrm{d}_x A = -\alpha A^n$ with solution $A^{(1-n)} = A_0^{(1-n)} - (1-n)\alpha x$ holds promise for a simple parameterization of wave attenuation in sea ice that includes the effects of both scattering and dissipation. But, it is just a parameterization.

5. Conclusion

Data Accessibility. Matlab codes and data files created for the numerical investigation reported here can be accessed through http://www.maths.otago.ac.nz/files/icebreakup/Data_breakup.zip.

Competing Interests. The author declares that he has no competing interests.

Funding. The author is indebted to ONR Departmental Research Initiative 'Sea State and Boundary Layer Physics of the Emerging Arctic Ocean' (award number N00014-131-0279), EU FP7 Grant (SPA-2013.1.1-06) and the University of Otago, for their support.

Acknowledgements. The author would also like to thank the Isaac Newton Institute for Mathematical Sciences for support and hospitality during the programme *The Mathematics of Sea Ice Phenomena* when work on this paper was undertaken. This work was supported by EPSRC grant number EP/K032208/1.

References

1. Squire VA, Dugan JP, Wadhams P, Rottier PJ, Liu AK. 1995 Of ocean waves and sea ice. *Annu. Rev. Fluid Mech.* **27**, 115–168.
2. Squire VA. 2007 Of ocean waves and sea-ice revisited. *Cold Reg. Sci. Technol.* **49**, 110–133.
3. Greenhill AG. 1887 Wave motion in hydrodynamics. *Am. J. Math.* **9**, 62–112.
4. Shackleton E. 1920 *South! The Story of Shackleton's Last Expedition 1914–1917*, chapter XII Elephant Island, pp. 225–243. New York: Macmillan.
5. Wadhams P, Squire VA, Ewing JA, Pascal RW. 1986 The effect of the marginal ice zone on the directional wave spectrum of the ocean. *J. Phys. Oceanogr.* **16**, 358–376.
6. Wadhams P, Squire VA, Goodman DJ, Cowan AM, Moore SC. 1987 The attenuation of ocean waves in the marginal ice zone. *J. Geophys. Res.* **93**, 6799–6818.
7. Fox C, Squire VA. 1994 On the oblique reflexion and transmission of ocean waves from shore fast sea ice. *Philos. T. Roy. Soc. A* **347**, 185–218.
8. Meylan MH, Squire VA. 1994 The response of ice floes to ocean waves. *J. Geophys. Res.* **99**, 899–900.
9. Montiel F, Squire VA, Bennetts LG. 2016 Attenuation and directional spreading of ocean wave spectra in the marginal ice zone. *J. Fluid Mech.* **790**, 492–522.
10. Montiel F, Squire VA. 2017 Modelling wave-induced sea ice break-up in the marginal ice zone. *Proc. R. Soc. Lon. Ser-A* **473**, 20170258.
11. Squire VA, Montiel F. 2016 Evolution of directional wave spectra in the marginal ice zone: A new model tested with legacy data. *J. Phys. Oceanogr.* **46**, 3121–3137.
12. Squire VA, Moore SC. 1980 Direct measurement of the attenuation of ocean waves by pack ice. *Nature* **283**, 365–368.

13. Airy GB. 1845 Tides and waves.
In *Encyclopaedia Metropolitana*, Mixed Sciences 3, chapter V, pp. 241–396. London: J. J. Griffin & Co.
14. Hegarty GM, Squire VA. 2008 A boundary integral method for the interaction of large amplitude waves with a compliant floating raft such as a sea-ice floe.
J. Eng. Math. **62**, 355–372.
15. Rogers WE, Thomson J, Shen HH, Doble MJ, Wadhams P, Cheng S. 2016 Dissipation of wind waves by pancake and frazil ice in the autumn beaufort sea.
J. Geophys. Res. **121**, 7991–8007.
16. Wang R, Shen HH. 2010 Gravity waves propagating into an ice-covered ocean: A viscoelastic model.
J. Geophys. Res. **115**.
C06024
17. Keller JB. 1998 Gravity waves on ice-covered water.
J. Geophys. Res. **103**, 7663–7670.
18. Shen HH, Squire VA. 1998 Wave damping in compact pancake ice fields due to interactions between ice cakes.
In *Antarctic Science Research Series* (ed. M Jeffries), volume 74, pp. 325–341. Washington D.C.: American Geophysical Union.
19. Wadhams P. 1973 Attenuation of swell by sea ice.
J. Geophys. Res. **78**, 3552–3563.
20. Carolis GD, Desiderio D. 2002 Dispersion and attenuation of gravity waves in ice: a two-layer viscous fluid model with experimental data validation.
Phys. Lett. A **305**, 399–412.
21. Newyear K, Martin S. 1999 Comparison of laboratory data with a viscous two-layer model of wave propagation in grease ice.
J. Geophys. Res. **104**, 7837–7840.
22. Weber JE. 1987 Wave attenuation and wave drift in the marginal ice zone.
J. Phys. Oceanogr. **17**, 2351–2361.
23. Liu AK, Mollo-Christensen E. 1988 Wave propagation in solid ice pack.
J. Phys. Oceanogr. **18**, 1702–1712.
24. Liu AK, Holt B, Vachon PW. 1991 Wave propagation in the marginal ice zone: model predictions and comparisons with buoy and synthetic aperture radar data.
J. Geophys. Res. **96**, 4605–4621.
25. Liu AK, Vachon PW, Peng CY, Bhogal A. 1992 Wave attenuation in the marginal ice zone during LIMEX.
Atmos. Ocean **30**, 192–206.
26. Cole DM, Johnson RA, Durell GD. 1998 Cyclic loading and creep response of aligned first-year sea ice.
J. Geophys. Res. **103**, 21,751–21,758.
27. Mosig JEM, Montiel F, Squire VA. 2015 Comparison of viscoelastic-type models for ocean wave attenuation in ice-covered seas.
J. Geophys. Res. **120**, 6072–6090.
28. Zhao X, Shen HH. 2015 Wave propagation in frazil/pancake, pancake, and fragmented ice covers.
Cold Reg. Sci. Technol. **113**, 71–80.
29. Zhao X, Shen HH. 2015 Ocean wave transmission and reflection by viscoelastic ice covers.
Ocean Model. **92**, 1–10.
30. Zhao X, Shen HH, Cheng S. 2015 Modeling ocean wave propagation under sea ice covers.
Acta Mech. Sinica **31**, 1–15.
31. Phillips OM. 1957 On the generation of waves by turbulent winds.
J. Fluid Mech. **2**, 417–445.
32. Kohout AL, Williams MJM, Dean SM, Meylan MH. 2014 Storm-induced sea-ice breakup and the implications for ice extent.
Nature **509**, 604–607.
33. Meylan MH, Bennetts LG, Kohout AL. 2014 In situ measurements and analysis of ocean waves.
Geophys. Res. Lett. **41**, 5046–5051.